

## ON-ROAD MAGNETIC EMISSIONS PREDICTION OF ELECTRIC CARS IN TERMS OF DRIVING DYNAMICS USING NEURAL NETWORKS

Ahmed M. Wefky<sup>1, \*</sup>, Felipe Espinosa<sup>1</sup>, Frank Leferink<sup>2</sup>, Alfredo Gardel<sup>1</sup>, and Robert Vogt-Ardatjew<sup>2</sup>

<sup>1</sup>University of Alcalá, Spain

<sup>2</sup>University of Twente, The Netherlands

**Abstract**—This paper presents a novel artificial neural network (ANN) model estimating vehicle-level radiated magnetic emissions of an electric car as a function of the corresponding driving pattern. Real world electromagnetic interference (EMI) experiments have been realized in a semi-anechoic chamber using Renault Twizy. Time-domain electromagnetic interference (TDEMI) measurement techniques have been employed to record the radiated disturbances in the 150 kHz–30 MHz range. Interesting emissions have been found in the range 150 kHz–3.8 MHz approximately. The instantaneous vehicle speed and acceleration have been chosen to represent the vehicle operational modes. A comparative study of the prediction performance between different static and dynamic neural networks has been done. Results showed that a Multilayer Perceptron (MLP) model trained with extreme learning machines (ELM) has achieved the best prediction results. The proposed model has been used to estimate the radiated magnetic field levels of an urban trip carried out with a Think City electric car.

### 1. INTRODUCTION

Vehicular emissions can be divided into three major classes: acoustic (audible) noise, exhaust emissions, i.e., gases as well as particles, and electromagnetic disturbances, i.e., conducted & radiated emissions. Several works have correlated the driving profile with exhaust emissions estimated from emission models or measured on a chassis dynamometer [1–8]. The influence of the driver behavior on the real

---

*Received 4 April 2013, Accepted 20 April 2013, Scheduled 19 May 2013*

\* Corresponding author: Ahmed Mohamed Wefky (awefky@depeca.uah.es).

world exhaust emissions has been analyzed using onboard exhaust measurement system in [9, 10]. The Electronics department at the University of Alcala (UAH) has developed an onboard measurement equipment to register the driver activity, vehicle state and road conditions as well as the corresponding exhaust emissions in real traffic conditions [11]. This was the starting point of a research line concerning the electromagnetic emissions of electric vehicles.

Electric drive vehicles have already been geared-up into mass production for energy conservation and environment protection purposes. EMI issues in this type of vehicles could become more severe than ever. Power converters usually operate at high frequencies and switch on high voltages as well as currents generating high level low frequency EMI. For example, both conducted and radiated magnetic field emissions due to a hybrid car have already exceeded the limits established by CISPR 25 [12]. Moreover, the results from the emissions tests carried out on 7 different electrically powered vehicles, with one exception, have exceeded the emission limits specified by 95/54/EC, CISPR 12, and 97/24/EC standards [13].

Real traffic electromagnetic radiated emissions due to vehicles have not been evaluated. Moreover, recent studies on automotive electromagnetic compatibility (EMC) have not adequately addressed the question of whether the driving regime affects the on-road radiated disturbances levels and frequency content. Furthermore, currently available automotive EMC standards, e.g., CISPR 12, SAE J551, 2004/104/EC, don't discuss the impact of the driving profile on the corresponding real world radiated interferences. Some EMC standards or directives, e.g., category 507 in the 4th edition of AECTP 500 [14], require measuring the radiated fields with the vehicle under test running at some constant speeds, i.e., steady state conditions. But, there are not standards requiring measurements during dynamic conditions like: idle (stationary), start-up, steady state cruise (high constant speed), various levels of acceleration/deceleration, normal braking, regenerative braking, and charging. Besides, there are no models capable of accurately correlating the vehicular radiated electromagnetic fields in real world with the driving characteristics. Recent studies have shown that the frequency content and intensity of the magnetic fields inside electric [15] and hybrid [16] vehicles are continuously changing with driving modes.

The problem is that measuring real traffic vehicular radiated fields in a direct way is a very complicated task because of the large size of antennas in low frequency ranges. Furthermore, such antenna would receive a lot of radiated waves from various interfering sources like: other vehicles, WiFi, GPS, Bluetooth, television broadcast, radio

broadcast, mobile networks, satellite networks, and power lines. In previous articles [17, 18], authors have already proposed a procedure of three steps to solve this problem as shown in Figure 1. In this paper, the same methodology has been applied on a Renault Twizy and a Think City.

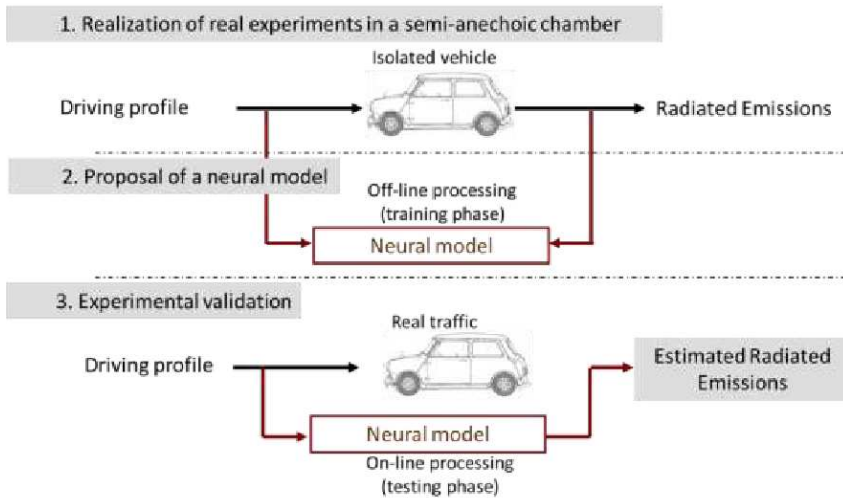


**Figure 1.** Procedure for estimating real traffic vehicular radiated emissions in terms of the driving profile.

Driving behavior has an effect on the output power of the motor and consequently its emissions. Driving dynamics and the corresponding radiated electromagnetic waves due to a certain vehicle under test should be registered simultaneously to study the relationship between them. The driving style can be described by a lot of variables such as: vehicle velocity, engine speed, linear acceleration, frontal inclination, regime engine, following distance, relative lane position, steering wheel angle, yaw angle, positions of pedals, use of accessories, and road grades (i.e., uphill or downhill) [19]. On-road measurement of some of these parameters is a straightforward task through the onboard diagnostic electronic system of the vehicle itself. Neural models have been developed to estimate the pedals activity in terms of the engine RPM, vehicle velocity, linear acceleration, and the frontal inclination in [20]. Moreover, a neural classifier has been proposed to determine the gear position as a function of the vehicle speed and the engine RPM in [21]. Some studies have used the vehicle velocity and acceleration to describe the operational modes of the vehicle [7, 8, 10, 22]. Whilst, other researchers have chosen the velocity as well as the product of

velocity and acceleration to characterize the driving regimes [2]. In this paper, the vehicle instantaneous speed and acceleration have been considered to represent the driving characteristics.

ANNs have been exploited in different EMC problems such as detection and identification of vehicles based on their unintended radiated emissions [23], target discrimination [24,25], calculation of multilayer magnetic shielding [26], estimating PCB configuration from EMI measurements [27], modeling of the integrated circuits immunity to conducted electromagnetic disturbances [28], recognition and identification of radiated EMI for shielding apertures [29], prediction of electromagnetic field in metallic enclosures [30], adaptive beamforming [31,32], PAD modeling [33], cross talk on PCB & radar cross-section of cylinders with apertures [34], and detection of dielectric cylinders buried in a lossy half-space [35]. The computational capabilities of ANNs have been already utilized to estimate exhaust concentrations as a function of traffic and meteorological variables in [36]. Unlike the computational electromagnetic (CEM) tools, ANNs can provide time varying inputs and deal with the problem as a black box.

TDEMI measurement systems provide some capabilities that could never be achieved using their traditional frequency domain counterpart like: improvement of impulsive emissions measurements and reduction of the measurement time. Nevertheless, there are two problems of the current time domain EMI measurement approaches: the limited dynamic range as well as the limited depth of memory to store a sufficient set of time domain data [37,38]. The measurement methodology followed in this paper is based on time domain methodology using digital oscilloscope to save the overall measurement time.

Most researchers interested in the measurement and analysis of electromagnetic emissions from electric driven vehicles concentrated on the magnetic field data [15,39–43]. Furthermore, recent measurements of electromagnetic emissions from a hybrid vehicle showed that the level of the electric radiated disturbances has been below the limits established by the CISPR 25 [12]. This is why in this paper, only the magnetic field data has been employed for training and testing the neural networks.

The contribution of this paper is to introduce a novel neural black-box model estimating the real time vehicle-level radiated EMI from an electric car in terms of the corresponding driving profile. The objective of that proposal is to quantify the change in real traffic radiated disturbances due to a corresponding perturbation in the driving dynamics. This can lead to suggesting traffic control

guidelines minimizing the vehicular radiated electromagnetic fields. For example, model-based traffic control determining the dynamic speed limits to reduce fuel consumption and exhaust emissions has been presented in [44]. Besides, such a model can be used for the comparison of EMI emissions from trips with different driving parameters. Furthermore, such type of models can be integrated into traffic network simulators to better understand the impact of traffic policies, including introduction of intelligent transport systems (ITS), on the electromagnetic environment.

The rest of the paper is organized as follows: Section 2 illustrates the measurement procedure followed in this work. Afterward, neural model development details are described in Section 3. Then, the experimental results are discussed in the fourth section. Finally, the conclusions and future works are included in the last section.

## 2. METHODOLOGY

The arrangement of the measurement system used in this article is outlined in Figure 2. Tests have been done inside a semi-anechoic chamber in the 150 kHz–30 MHz range. Electric as well as magnetic fields have been measured. The antennas have been put at a distance of 1 meter behind the car under test; because in this case the motor was in the rear part of the car. A loop antenna has been used to measure magnetic radiated EMI signals as shown in Figure 3. Anti-aliasing filters weren't needed because the bandwidth of the antenna was 150 kHz–30 MHz.

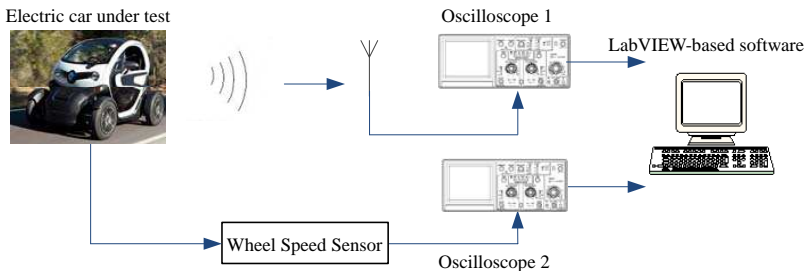


**Figure 2.** Schematic diagram of the measurement setup.

EMI signals have been sampled at 125 MHz, the sweep duration, or the capture time, was 100  $\mu$ s, and time between sweeps, i.e., sweeping time, was 1 second. The relationship between sweeping, sampling and capture times has been explained in [17]. It's noteworthy that authors are not interested in absolute values of radiated emissions.



**Figure 3.** ROHDE & SCHWARZ loop antenna used in the measurements.

The key point in this work is to quantify the relative change of radiated disturbances as a response to changes in the driving variables.

The driving profile has been registered by measuring the wheel rotational speed. The vehicle has been jacked up some centimeters from the ground by means of wood supports. A rely as can be seen in Figure 4(a) has been used to design the speed measurement system. More details of the wheel speed measurement circuit are illustrated in Figure 4(b). The velocity of the car has been changed manually. Six magnets have been fixed along the circumference of one of the rear wheels with a separation of 60 degrees approximately. This electronic

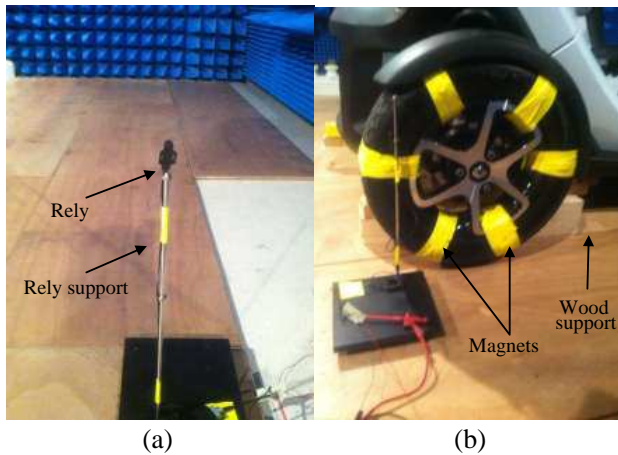


**Figure 4.** Wheel speed measurement system. (a) Magnetic sensor (rely). (b) Speed measurement circuit.

system has been fixed near the wheel such that the rely conducts when a magnet passes. The wheel speed signal has been sampled by another oscilloscope at a rate of 10 kHz. The sweep duration was 500 ms, and time between sweeps was also 1 second. These values for the speed measurement system have been chosen by trial and error.

A labVIEW software application has been designed to synchronize and save the sweeps of the EMI and speed signals. At the end of each experiment, two matrices are available in the database of the PC: EMI matrix and speed matrix. The rows represent the time-domain sweeps and the columns represent the samples within sweeps.

With respect to the EMI signals matrix: samples of electric or magnetic field are measured in Volts. In order to take into account the errors due to the antenna factor and the cable losses, Fast Fourier Transform (FFT) is applied to each sweep to convert it from time to frequency domain. To calculate the field intensity in dBuV/m, Eq. (1) should be considered where  $V$  is the FFT point to be corrected,  $F$  is the antenna factor and  $L$  is the cable losses. It has been found that the magnetic radiated emissions are concentrated in the 150 kHz–3.8 MHz frequency range. Thus; sweep average value has been easily calculated by averaging the sweep instantaneous field values in that range.

$$E \text{ (dBuV/m)} = 20 * \log(V) + 120 + F \text{ (dB/m)} + L \text{ (dB)} \quad (1)$$

On the other hand, the speed matrix contains samples of the digital signal resulting from the sensor. To calculate the sweep instantaneous speed, Eq. (2) should be considered where  $D$  is the wheel diameter in meters,  $C$  is the number of pulses per sweep,  $N$  is the number of pulses per turn, in this case 6, and  $T$  is the sweep duration in Seconds. With the acquired instantaneous speed data, instantaneous acceleration has been calculated by forward finite difference method.

$$\text{speed (km/h)} = \frac{C}{N} \frac{1}{T} \frac{\pi D}{1000} 3600 \quad (2)$$

### 3. ANN MODEL DEVELOPMENT

ANNs have been widely used in various applications in recent years. Since the basic back-propagation learning algorithm is too slow for most practical applications, there have been extensive research efforts to accelerate its convergence. In this work, different gradient-descent variations of the backpropagation algorithm have been considered like Levenberg-Marquardt (LM) [45], Scaled Conjugate Gradient (SCG) [46], One Step Secant (OSS) [47], and Quasi-Newton BFGS [48].

ELM is considered a recently emerging learning algorithm that overcomes some challenges faced by the conventional backpropagation

training such as: slow learning speed, trivial human intervene, local minima, and poor computational scalability [49]. ELM is designed for single hidden layer feedforward neural network topology. The ELM-trained networks have been proven to satisfy the universal approximation property [50]. This learning algorithm has been exploited to train the MLP neural network in this paper.

Couple of reasons can lead to the failure of a given ANN. Firstly; improper initialization can cause the model parameters to fail to converge to the proper values. On the other hand, an insufficient number of hidden neurons can lead to the inability of the given model to implement the desired function. In this work, to avoid the first possibility, each neural model was trained and tested 10 times. The network architecture with the lowest root mean square error (RMSE) on the testing data set has been chosen. The RMSE has been calculated according to Eq. (3) where  $N$  is the size of the testing dataset,  $P$  is the vector of predicted values by the model,  $O$  is the vector of observed or measured values by the measurement system. With respect to the second reason, there is no theory yet to explain how to choose the optimal number of hidden neurons to approximate any given function. If the hidden neurons are too few, a high training error and high generalization error would result due to under-fitting. On the contrary, if the hidden neurons are too many, there would be a low training error, but there would still be a high generalization error due to over-fitting. In most situations, the best way to determine the optimum size of the hidden layer is to train several networks and estimate the generalization error of each [51, 52]. In this paper, the network growing technique [51] is applied by sequentially adding hidden neurons from 1 to 10 comparing the testing RMSE.

$$\text{RMSE} = \left[ \frac{1}{N} \sum_{i=1}^N (P_i - O_i)^2 \right]^{1/2} \quad (3)$$

In general, two types of neural models based on number of inputs have been tested. All models have only one output that's the level of radiated emissions in dBuV/m. The first type of models has only single input: the speed while the other type of models has two inputs: speed and acceleration. Static and dynamic neural architectures have been employed in this paper. Static topologies include the linear layer, MLP, cascade [53], and double hidden layer networks. The linear layer contained always one neuron and has been trained with the least mean square (LMS) algorithm [52]. The cascade feedforward structure is the same as the MLP with an extra connection form the inputs to the output layer. Dynamic models include: focused time delay network (FTDN), Distributed time delay network (DTDN), layer recurrent

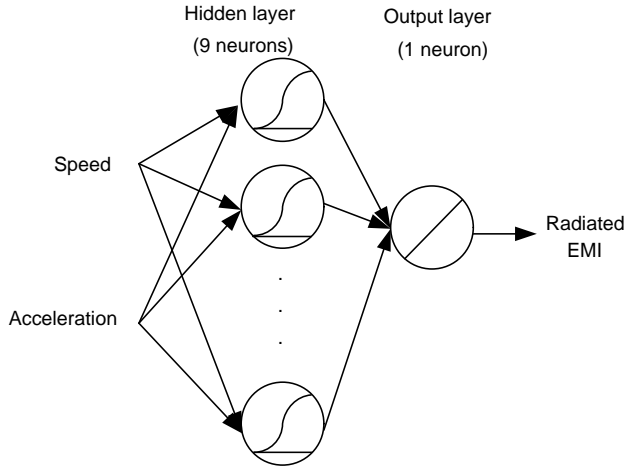
or Elman network (LRN), and nonlinear autoregressive with external input (NARX) network. The FTDN structure contains delay elements at the input of the hidden layer. The DTDN topology contains delay elements at the input of both the hidden and output layer. All the networks except for the linear layer use log-sig hidden layer (s) and linear output layer.

Table 1 demonstrates the best results obtained from testing all the neural network topologies. It also points out that the relation between the instantaneous vehicle operational variables and the corresponding radiated EMI levels is nonlinear because of the failure of the linear layer to model this relationship. Moreover, the effectiveness and robustness of the ELM algorithm can be noticed comparing the training times needed to achieve similar performance. Thorough analysis of the results given in this table suggests that two models can be candidates to be used for estimating the radiated emissions in terms of the driving characteristics: the single input NARX model and the double inputs MLP model. This result is logical because the problem of interest is a dynamic one. That's the current level of the radiated emissions depends on the corresponding value of the speed as well as its history. Consequently, if only the speed signal is considered as an input, a dynamic model will give the best estimation results. However, if both the speed and its derivative are considered, a static model will give the best results. Authors prefer to choose the double-input ELM-trained MLP model because of its short training time relative to the single-

**Table 1.** Testing results of the different neural models.

Inputs	Network Type	Topology	Learning Function	Delays (Input / Feedback)	Neurons ( $h_1/h_2$ )	RMSE	Training Time
Speed	Static	Linear layer	LMS	X	1	8.7245	40 m
		MLP	ELM		3	4.822	5 h 35 m
		Double layer	SCG		2   2	4.8361	2 d 20 h
		Cascade	BFGS		2	4.8290	2 h 6 m
	Dynamic	FTDN	LM	1	5	4.8499	1 h 7 m
		DTDN	LM	1   1	3	4.8503	5 d 1 h 17 m
		LRN	SCG	1	2	4.8434	1 d 7 h
		NARX	BFGS	2   1	2	4.7934	5 h 56 m
Speed & Acceleration	Static	Linear layer	LMS	X	1	8.8006	45 m
		MLP	ELM		9	4.7425	1 h 40 m
		Double layer	OSS		2   6	4.8388	19 h
		Cascade	SCG		2	4.8996	8 h
	Dynamic	FTDN	LM	1	4	4.8463	1 h 28 m
		DTDN	OSS	1   1	2	4.8574	1 d 15 h
		LRN	OSS	1	2	4.8481	1 d 22 h
		NARX	SCG	2   2	2	4.8625	20 h 35 m

input NARX model as can be seen in the latest column of Table 1. Figure 5 shows the schematic diagram of the best model.



**Figure 5.** Topology of the selected model.

#### 4. RESULTS

Three types of velocity profiles have been applied to the Renault Twizy: pulse, steps, and elementary European driving cycle (EEDC) profiles as depicted in Figures 6 & 7. The EEDC profile is a standard driving cycle that is usually used with internal combustion vehicles to evaluate the exhaust emissions and fuel consumption. The aim of the pulse profile is to analyze the effect of acceleration and deceleration on the corresponding radiated interferences. The car has been also

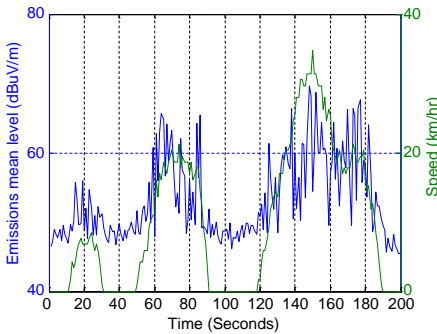


**Figure 6.** Training data (EEDC profile).

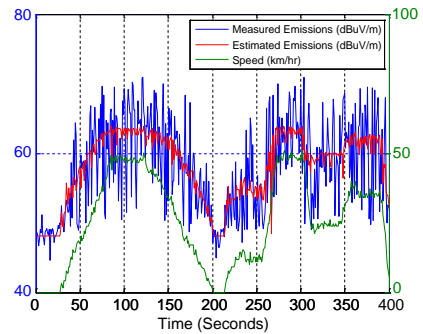


**Figure 7.** Testing data (pulse and steps profiles) & estimation results.

subjected to the steps profile in order to study the influence of the sharp accelerations and constant speeds on the corresponding radiated disturbances. Both the steps and pulse profiles can simulate different interurban driving behaviors up to 50 km/h taking into account that the maximum speed of the Twizy was 80 km/h. Moreover, the EEDC profile approximates the standard urban driving characteristics.

Magnetic field data of the EEDC profile has been exploited for training as shown in Figure 6 while the data of the two other profiles has been utilized for testing as depicted in Figure 7. Moreover, this figure also demonstrates the emissions estimated by the model shown in Figure 5. The model can successfully distinguish between 4 different levels of different speeds as well as it responds reasonably to moderate and sharp accelerations. Figure 8 shows that although the testing dataset contained unseen speed values, e.g., more than 35 km/h, during the training phase, the model could accurately predict the corresponding level of magnetic emissions as can be observed in Figure 7.

Generally, magnetic emission levels increased with the increase of the vehicle speed. Maximum levels of magnetic interferences have been detected during both acceleration in urban driving represented by the EEDC training dataset and cruising in the testing dataset as can be concluded from Figure 8. This is because at acceleration and cruising, vehicles have to deliver more power to accelerate and maintain constant speed respectively thus generating more radiated emissions. The same figure also shows that the idling emissions are the lowest as expected; as a small amount of power is needed to maintain the engine operation.

In order to complete the proposed solution in [17, 18], the urban

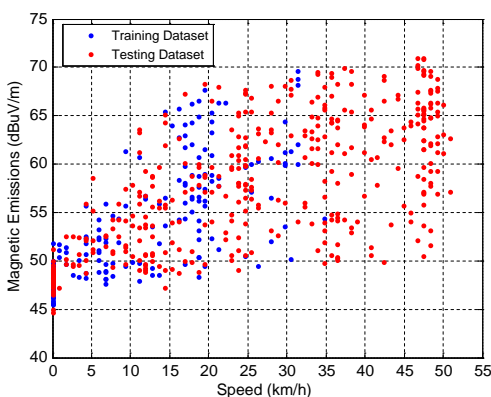


**Figure 8.** Levels of magnetic emissions versus the instantaneous vehicle speed.



**Figure 9.** Map image of the trip in Alcalá de Henares (Madrid).

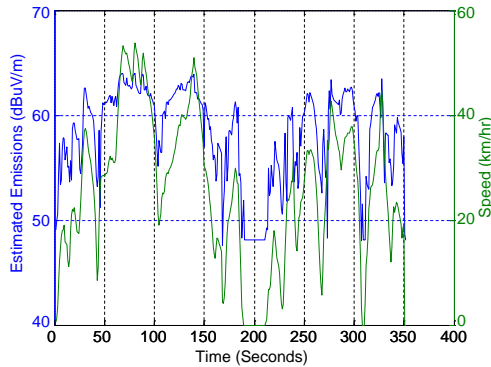


**Figure 10.** Estimation of the Think City radiated emissions.

trip illustrated in Figure 9 has been realized with a Think City in Alcalá de Henares (Madrid) recording only the on-road car speed by means of an onboard Differential Global Positioning System (DGPS) device. Then the instantaneous speed and calculated acceleration values during the trip have been applied to the proposed model in this paper to predict the corresponding magnetic radiated emissions as shown in Figure 10.

## 5. CONCLUSIONS

The paper describes a proposal for the prediction of vehicular electromagnetic pollutant emissions in real traffic conditions. First of all, an ELM-trained MLP ANN has been developed to estimate

the real time radiated disturbances of electric vehicles in terms of the instantaneous speed and acceleration. Experiments had been done registering the speed and radiated emissions of a Renault Twizy using a TDEMI measurement methodology. The higher levels of magnetic disturbances have been detected during both cruising in extra-urban driving and acceleration mode in urban driving. Finally, the validated model has been employed to predict the on-road radiated interferences measuring only the driving profile during an urban trip with a Think City. The main contribution of the paper is the implementation of an alternative solution for the complex task of directly measuring the radiated EMI interferences from road electric transport. In this way, comparative studies and policies can be applied in order to evaluate and minimize the environmental effect of electric transport, mainly in urban areas.

As future work, authors are interested on extending this methodology to other transport units as well as on tackling with conducted emissions and their relationship with the radiated ones as a function of the driving variables.

## ACKNOWLEDGMENT

This work has been partially funded by the Spanish Ministry of Science and Innovation through the SIGVE project (Ref. IPT-440000.2010-0020) and by the FPU grant of the Spanish Ministry of Education (Ref. AP2008-02506).

## REFERENCES

1. Hansen, J. Q., M. Winther, and S. C. Sorenson, "The influence of driving patterns on petrol passenger car emissions," *Science of the Total Environment*, Vol. 169, Nos. 1–3, 129–139, 1995.
2. Joumard, R., et al., "Hot passenger car emissions modelling as a function of instantaneous speed and acceleration," *Science of the Total Environment*, Vol. 169, Nos. 1–3, 167–174, 1995.
3. Sjödin, Å and M. Lenner, "On-road measurements of single vehicle pollutant emissions, speed and acceleration for large fleets of vehicles in different traffic environments," *Science of the Total Environment*, Vol. 169, Nos. 1–3, 157–165, 1995.
4. Barth, M., et al., "Analysis of modal emissions from diverse in-use vehicle fleet," *Transportation Research Record: Journal of the Transportation Research Board*, Vol. 1587, 73–84, 1997.

5. Nesamani, K. S. and K. P. Subramanian, "Impact of real-world driving characteristics on vehicular emissions," *JSME International Journal Series B: Fluids and Thermal Engineering*, Vol. 49, No. 1, 19–26, 2006.
6. Washington, S., J. Wolf, and R. Guensler, "Binary recursive partitioning method for modeling hot-stabilized emissions from motor vehicles," *Transportation Research Record: Journal of the Transportation Research Board*, Vol. 1587, 96–105, 1997.
7. Barth, M. J., et al., "Development of a comprehensive modal emissions model," Monograph Record, 2000.
8. Sorenson, S. C., et al., "Individual and public transportation — Emissions and energy consumption models," Lyngby, 1992.
9. Holmén, B. A. and D. A. Niemeier, "Characterizing the effects of driver variability on real-world vehicle emissions," *Transportation Research Part D: Transport and Environment*, Vol. 3, No. 2, 117–128, 1998.
10. Tong, H., W. Hung, and C. Cheung, "On-road motor vehicle emissions and fuel consumption in urban driving conditions," *Journal of the Air & Waste Management Association*, Vol. 50, No. 4, 543–554, 2000.
11. Espinosa, F., et al., "Design and implementation of a portable electronic system for vehicle-driver-route activity measurement," *Measurement*, Vol. 44, No. 2, 326–337, 2011.
12. Silva, F. and M. Aragon, "Electromagnetic interferences from electric/hybrid vehicles," *2011 XXXth URSI General Assembly and Scientific Symposium*, 1–4, 2011.
13. Ruddle, A. R., D. A. Topham, and D. D. Ward, "Investigation of electromagnetic emissions measurements practices for alternative powertrain road vehicles," *2003 IEEE International Symposium on Electromagnetic Compatibility*, Vol. 2, 543–547, 2003.
14. Agency, N. S., *Allied Environmental Conditions and Tests Publication, AECTP 500*, 4th edition, January 2011.
15. Ptitsyna, N. and A. Ponzetto, "Magnetic fields encountered in electric transport: Rail systems, trolleybus and cars," *2012 International Symposium on Electromagnetic Compatibility (EMC EUROPE)*, 1–5, 2012.
16. Halgamuge, M. N., C. D. Abeyrathne, and P. Mendis, "Measurement and analysis of electromagnetic fields from trams, trains and hybrid cars," *Radiation Protection Dosimetry*, Vol. 141, No. 3, 255–268, 2010.
17. Wefky, A., et al., "Electrical drive radiated emissions estimation

- in terms of input control using extreme learning machines,” *Mathematical Problems in Engineering*, Vol. 2012, 11, 2012.
18. Wefky, A. M., et al., “Modeling radiated electromagnetic emissions of electric motorcycles in terms of driving profile using mlp neural networks,” *Progress In Electromagnetics Research*, Vol. 135, 231–244, 2013.
  19. Miyajima, C., et al., “Cepstral analysis of driving behavioral signals for driver identification,” *2006 IEEE International Conference on Acoustics, Speech and Signal Processing, ICASSP 2006 Proceedings*, 2006.
  20. Wefky, A. M., et al., “Alternative sensor system and MLP neural network for vehicle pedal activity estimation,” *Sensors*, Vol. 10, No. 4, 3798–3814, 2010.
  21. Wefky, A., et al., “Comparison of neural classifiers for vehicles gear estimation,” *Applied Soft Computing*, Vol. 11, No. 4, 3580–3599, 2011.
  22. Ahn, K., et al., “Estimating vehicle fuel consumption and emissions based on instantaneous speed and acceleration levels,” *Journal of Transportation Engineering*, Vol. 128, No. 2, 182–190, 2002.
  23. Dong, X., et al., “Detection and identification of vehicles based on their unintended electromagnetic emissions,” *IEEE Transactions on Electromagnetic Compatibility*, Vol. 48, No. 4, 752–759, 2006.
  24. Tsai, C. Y., E. J. Rothwell, and K. M. Chen, “Target discrimination using neural networks with time domain or spectrum magnitude response,” *Journal of Electromagnetic Waves and Applications*, Vol. 10, No. 3, 341–382, 1996.
  25. Atkins, R. G., R. T. Shin, and J. A. Kong, “A neural network method for high range resolution target classification,” *Progress In Electromagnetics Research*, Vol. 4, 255–292, 1991.
  26. Koroglu, S., et al., “An approach to the calculation of multilayer magnetic shielding using artificial neural network,” *Simulation Modelling Practice and Theory*, Vol. 17, No. 7, 1267–1275, 2009.
  27. Aunchaleevarapan, K., K. Paithoonwatanakij, W. Khan-Ngern, and S. Nitta, “Novel method for predicting PCB configurations for near field and far field radiated EMI using a neural network,” *IEICE Trans. Commun.*, Vol. E86-B, No. 4, 1364–1376, 2003.
  28. Chahine, I., et al., “Characterization and modeling of the susceptibility of integrated circuits to conducted electromagnetic disturbances up to 1 GHz,” *IEEE Transactions on Electromagnetic Compatibility*, Vol. 50, No. 2, 285–293, 2008.

29. Sujintanarat, P., P. Dangkhom, S. Chaichana, K. Aunchaleevapan, and P. Teekaput, "Recognition and identification of radiated EMI for shielding aperture using neural network," *PIERS Online*, Vol. 3, No. 4, 444–447, 2007.
30. Luo, M. and K.-M. Huang, "Prediction of the electromagnetic field in metallic enclosures using artificial neural networks," *Progress In Electromagnetics Research*, Vol. 116, 171–184, 2011.
31. Zaharis, Z. D., K. A. Gotsis, and J. N. Sahalos, "Comparative study of neural network training applied to adaptive beamforming of antenna arrays," *Progress In Electromagnetics Research*, Vol. 126, 269–283, 2012.
32. Zaharis, Z. D., K. A. Gotsis, and J. N. Sahalos, "Adaptive beamforming with low side lobe level using neural networks trained by mutated boolean PSO," *Progress In Electromagnetics Research*, Vol. 127, 139–154, 2012.
33. Li, X. and J. Gao, "Pad modeling by using artificial neural network," *Progress In Electromagnetics Research*, Vol. 74, 167–180, 2007.
34. Al Salameh, M. S. and E. T. Al Zuraiqi, "Solutions to electromagnetic compatibility problems using artificial neural networks representation of vector finite element method," *IET Microwaves, Antennas & Propagation*, Vol. 2, No. 4, 348–357, 2008.
35. Bermiani, E., S. Caorsi, and M. Raffetto, "An inverse scattering approach based on a neural network technique for the detection of dielectric cylinders buried in a lossy half-space," *Progress In Electromagnetic Research*, Vol. 26, 69–90, 2000.
36. Khare, M. and S. M. S. Nagendra, *Artificial Neural Networks in Vehicular Pollution Modelling*, Springer, 2007.
37. Winter, W. and M. Herbrig, "Time domain measurements a novel method for qualification of electronics," *2010 15th International Conference on Microwave Techniques (COMITE)*, 19–24, 2010.
38. Winter, W. and M. Herbrig, "Time domain measurements in automotive applications," *2009 IEEE International Symposium on Electromagnetic Compatibility*, 109–115, 2009.
39. Karabetsos, E., et al., "EMF measurements in hybrid technology cars," *Proceedings of 6th International Workshop on Biological Effects of Electromagnetic Fields*, Istanbul, 2010.
40. Concha Moreno-Torres, P., et al., "Evaluation of the magnetic field generated by the inverter of an electric vehicle," *IEEE Transactions on Magnetics*, Vol. 49, No. 2, 837–844, 2013.

41. Berisha, S., et al., "Magnetic field generated from different electric vehicles," SAE Technical Paper 951934, 1995.
42. Ptitsyna, N., et al., "Analysis of magnetic fields onboard electric transport systems in regard to human exposure," *2012 International Symposium on Electromagnetic Compatibility (EMC EUROPE)*, 1–5, 2012.
43. Kopytenko, Y. A., et al., "Monitoring and analysis of magnetic fields onboard transport systems: Waveforms and exposure Assessment," *2007 7th International Symposium on Electromagnetic Compatibility and Electromagnetic Ecology*, 331–333, 2007.
44. Zegeye, S., et al., "Model-based traffic control for the reduction of fuel consumption, emissions, and travel time," *12th IFAC Symposium on Control in Transportation Systems*, 149–154, 2009.
45. Hagan, M. T. and M. B. Menhaj, "Training feedforward networks with the Marquardt algorithm," *IEEE Transactions on Neural Networks*, Vol. 5, No. 6, 989–993, 1994.
46. Møler, M. F., "A scaled conjugate gradient algorithm for fast supervised learning," *Neural Networks*, Vol. 6, No. 4, 525–533, 1993.
47. Battiti, R., "First-and second-order methods for learning: Between steepest descent and Newton's method," *Neural Computation*, Vol. 4, No. 2, 141–166, 1992.
48. Setiono, R. and L. C. K. Hui, "Use of a quasi-Newton method in a feedforward neural network construction algorithm," *IEEE Transactions on Neural Networks*, Vol. 6, No. 1, 273–277, 1995.
49. Huang, G.-B., D. Wang, and Y. Lan, "Extreme learning machines: A survey," *International Journal of Machine Learning and Cybernetics*, Vol. 2, No. 2, 107–122, 2011.
50. Huang, G.-B., L. Chen, and C.-K. Siew, "Universal approximation using incremental constructive feedforward networks with random hidden nodes," *IEEE Transactions on Neural Networks*, Vol. 17, No. 4, 879–892, 2006.
51. Haykin, S. S., *Neural Networks: A Comprehensive Foundation*, Prentice Hall, 1999.
52. Hagan, M. T., H. B. Demuth, and M. H. Beale, *Neural Network Design*, PWS Pub., 1996.
53. Demuth, H. and M. Beale, "Neural network toolbox: For use with MATLAB®," Mathworks, 2001.